Fast Switching in Magnetic Tunnel Junctions with Double Barrier Layer

Alexander Makarov, Viktor Sverdlov, Dmitry Osintsev, and Siegfried Selberherr

TU Wien, Institute for Microelectronics
Gußhausstraße 27-29
A-1040 Wien, Austria
Phone: +43(1)58801-36028 E-mail: Makarov@iue.tuwien.ac.at

1. Introduction

Memory cells based on electric charge storage, such as flash memory, are rapidly approaching the physical limits of scalability. The spin transfer torque random access memory (STTRAM) is one of the promising candidates for future universal memory [1-6]. The reduction of the current density required for switching and the increase of the switching speed are among the most important challenges in this area. Measurements performed in [4] showed a decrease in the critical current density for the penta-layer magnetic tunnel junction (MTJ) compared with the tri-layer MTJ. To achieve symmetric switching in asymmetric MTJs an external in-plane compensating magnetic field has to be introduced [4]. By numerically investigating the dynamics of the switching process in a MTJ composed of five layers we present the methodology on how to achieve symmetric switching without an external magnetic field by properly engineering the nanopillar geometry.

2. Model Description

Our micromagnetic simulations are based on the magnetization dynamics described by the Landau-Lifschitz-Gilbert equation:

$$\frac{dm}{dt} = -\frac{\gamma}{1+\alpha^2} \cdot \left((m \times h_{eff}) + \alpha \cdot \left[m \times (m \times h_{eff}) \right] \right)$$
$$+ \frac{g\mu_B j}{e\gamma M_s d} \cdot \left(g_1(\theta_1) \cdot (\alpha \cdot (m \times p_1) - [m \times (m \times p_1)]) \right) \quad (1)$$
$$- g_2(\theta_2) \cdot (\alpha \cdot (m \times p_2) - [m \times (m \times p_2)])),$$

Here, γ is the gyromagnetic ratio, α is the Gilbert damping parameter, g is the gyromagnetic splitting factor, μ_B is Bohr's magneton, j is the current density, e is the electron charge, d is the thickness of the free layer, $m=M/M_s$ is the position dependent normalized vector of the magnetization in the free layer, $p_1=M_{p1}/M_{sp1}$ and $p_2=M_{p2}/M_{sp2}$ are the normalized magnetizations in the first and second pinned layers, respectively. M_s, M_{sp1}, and M_{sp2} are the saturation magnetizations of the free layer, the first pinned layer, and the second pinned layer, correspondingly. We use the Slonczewski's expressions for the giromagnetic splitting factor in the MTJ with a dielectrical layer [7]

$$g_1(\theta) = 0.5 \cdot \eta \cdot \left[1 + \eta^2 \cdot \cos(\theta) \right]^{-1} \quad (2)$$

and with a metal layer [8]

$$g_2(\theta) = \left[-4 + (1+\eta)^3 (3 + \cos(\theta))/4\eta^{3/2} \right]^{-1} \quad (3)$$

between the ferromagnetic contacts, respectively. In the penta-layer structure the two spin torques are acting independently on the two opposite interfaces of the free ferromagnetic layer provided its thickness is larger than the scale on which the electron spins entering into the ferromagnet become aligned to the ferromagnet's magnetization. The local effective field is calculated as:

$$h_{eff} = h_{ext} + h_{ani} + h_{exch} + h_{demag} + h_{th} + h_{amp} + h_{ms}, \quad (4)$$

In addition to the standard external h_{ext} and the anisotropic h_{ani} micromagnetic contributions considered in [9] we also include the exchange h_{exch} and demagnetizing h_{demag} fields. h_{th} is a thermal field [10], h_{amp} is the Ampere field [11], and h_{ms} is the magnetostatic coupling between the pinned layers and the free layer.

3. Results

All simulations are performed for the nanopillar proposed in [4]. The geometry of the nanopillar is defined as CoFe(8nm)/ AlOx(0.7nm)/ Py(4nm)/ Cu(6nm)/ CoFe(5nm), with an elliptical crossection (major axes are 90nm and 35nm, correspondingly). The other parameters of our simulations are: T=77K, γ=2.3245·10^5m/(A·s), α=0.01, A=1.3·10^{-11}J/m, M_s=644·10^3A/m, M_{sp}=1.15·10^6A/m and η_1=0.3 and η_2=0.35 for the MTJ with the dielectric spacer and the metal spacer, respectively.

We investigate the influence of the thicknesses of the fixed layers on the switching times between the two stable configurations of the free magnetic layer. The corresponding dependence is shown in Fig.1. Each point is a result of statistical averaging with respect to 15 different realizations of the switching process. Fig.1 demonstrates that the values of the switching time from the parallel to the anti-parallel configuration and vice versa depend strongly on the fixed layer thickness. The fastest and the most symmetric switching is achieved when the fixed layer thickness is around 9-10nm.

The reason for this result is illustrated in Fig.2: the in-plane component of the magnetostatic exchange field is nearly compensated for a thickness of the fixed layer around 10nm. A more precise analysis reveals that the value of the most symmetric switching does not coincide with the maximum compensation of the in-plane projection of the magnetostatic field achieved, when the thickness of the second layer is about 11-12nm as shown in Fig. 3.

To find the reason for this discrepancy we stress that by varying the thickness of the fixed layer one can only com-
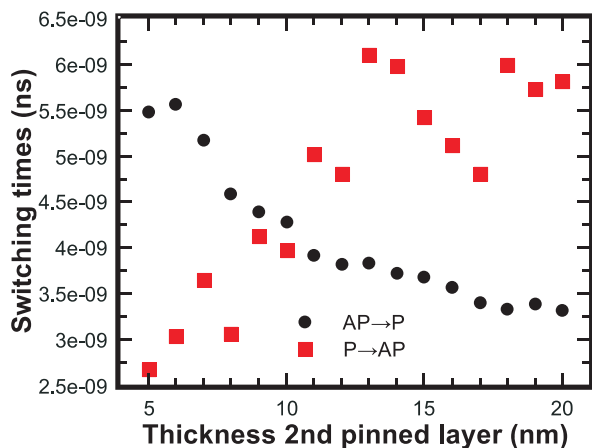
Fig. 1. Dependence of the switching times between the two stable configurations on the thickness of the second fixed magnetic layer. The thickness of the first fixed magnetic layer is 8nm.

pensate the in-plane component of the magnetostatic exchange field. At the same time the field projection perpendicular to the plane is not compensated (see Fig.2). The absolute value of the average filed orthogonal to the plane of the free layer is also shown in Fig.3. This field component facilitates switching [12] and explains the shift of the optimal point away from the point of the best compensation of the in-plane field.

4. Conclusions

Magnetic tunnel junctions with three magnetic layers are studied by means of extensive micromagnetic calculations. By varying the thicknesses of the side fixed ferromagnetic layers and/or the separation between them one can modulate the switching time and achieve an almost symmetric switching. Our simulations also highlight the importance of the field acting perpendicular to the plane. This field facilitates switching. The proposed method can be used for performance optimization of STTRAM devices.

References
[1] P. M. Braganca et al., Appl. Phys. Lett., **87** (2005), 112507.
[2] M. Iwayama *et al.*, J. Appl. Phys., **103** (2008), 07A720.
[3] H. Meng *et al.*, Appl. Phys. Lett., **88** (2006), 082504.
[4] G. D. Fuchs *et al.*, Appl. Phys. Lett., **86** (2005), 152509.
[5] T. Devolder *et al.*, Appl. Phys. Lett., **86** (2005), 062505.
[6] Y. Huai *et al.*, Appl. Phys. Lett., **87** (2005), 2225.
[7] J. Slonczewski, Phys. Rev. B, **71** (2005), 024411.
[8] J. Slonczewski, J. Magn. Magn. Mater., **159** (1996), L1.
[9] N.N. Mojumdar *et al.*, J. Appl. Phys., **108** (2010), 104306.
[10] G. Finocchio *et al.*, J. Appl. Phys., **99** (2006), 08G522.
[11] L. Torres *et al.*, IEEE Trans. Magn., **39** (2003).
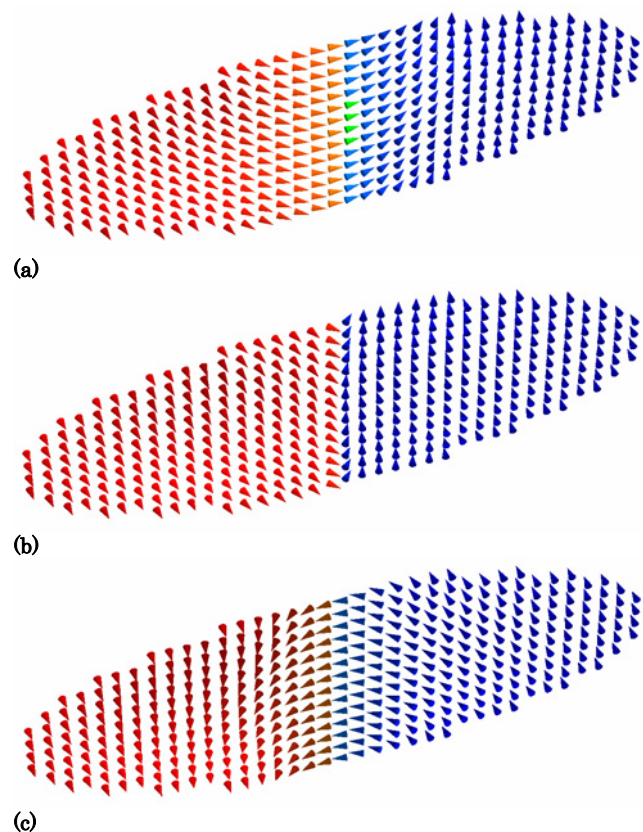[12] M. Carpentieri, J. Appl. Phys., **103** (2008), 07B117.

Fig. 2. Snapshots of the magnetostatic exchange magnetic field between the fixed layers and the free magnetic layer at the plane of the free layer: (a) the thickness of the second fixed layer is 5nm; (b) 9nm; (c) 20nm.
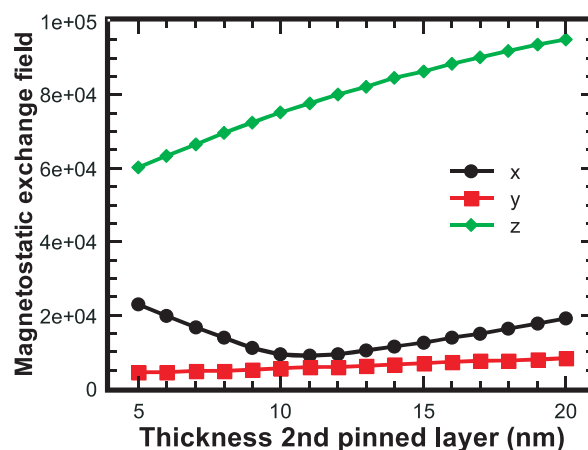

Fig. 3. Dependence of the absolute values of different components of the averaged magnetostatic field acting on the free magnetic layer on the thickness of the second fixed magnetic layer. The thickness of the first magnetic layer is fixed at 8nm.